

# Effect of probe pulse duration in picosecond ultrasonics

Cite as: Appl. Phys. Lett. **120**, 202201 (2022); doi: [10.1063/5.0093321](https://doi.org/10.1063/5.0093321)

Submitted: 28 March 2022 · Accepted: 9 May 2022 ·

Published Online: 16 May 2022



View Online



Export Citation



CrossMark

Yuchen Liu,<sup>1</sup> Jian Yin,<sup>2,3</sup> Xutang Tao,<sup>2,3</sup>  Arkady Yartsev,<sup>1,a)</sup>  and Pierre-Adrien Mante<sup>1,a)</sup> 

## AFFILIATIONS

<sup>1</sup>Division of Chemical Physics and NanoLund, Lund University, Lund, Sweden

<sup>2</sup>State Key Laboratory of Crystal Materials, Shandong University, Jinan, People's Republic of China

<sup>3</sup>No. 18 Research Institute of China Electronics Technology Group Corporation, Beijing, People's Republic of China

<sup>a)</sup>Authors to whom correspondence should be addressed: [arkady.yartsev@chemphys.lu.se](mailto:arkady.yartsev@chemphys.lu.se) and [pierre-adrien.mante@chemphys.lu.se](mailto:pierre-adrien.mante@chemphys.lu.se)

## ABSTRACT

Picosecond ultrasonics is a powerful tool for nanoscale metrology, giving access to dimensions and mechanical, thermal, and optical properties of nanomaterials. By monitoring the temporal evolution of the interaction of light with coherent acoustic phonons, also known as Brillouin oscillations, phonon lifetime and optical absorption can be measured. However, the extraction of these quantities can be inaccurate due to the common assumption of the infinite coherence length of probe pulses. Here, we demonstrate the effect of probe pulse duration on picosecond ultrasonic measurements numerically and experimentally. We establish a model that shows how the probe coherence length affects the measured signal loss and how we can overcome this limitation and measure an upper limit of the acoustic attenuation factor. The model is verified experimentally on a GaAs bulk substrate by varying the probe pulse duration, showing a strong effect for sub-100 fs pulses. Finally, we applied to  $\text{CH}_3\text{NH}_3\text{PbBr}_3$ , where we reveal a high acoustic attenuation factor, which is in line with recent claims of strong anharmonicity in halide perovskites.

© 2022 Author(s). All article content, except where otherwise noted, is licensed under a Creative Commons Attribution (CC BY) license (<http://creativecommons.org/licenses/by/4.0/>). <https://doi.org/10.1063/5.0093321>

The study of the attenuation of subterahertz to THz acoustic phonons has attracted considerable attention because of their important role in numerous physical processes.<sup>1–4</sup> Acoustic attenuation reflects energy dissipation and, as such, not only plays an important role in heat transport<sup>3</sup> but also opens a window into the dynamics of the structure of materials.<sup>5</sup> Finally, understanding and increasing the lifetime of high frequency acoustic phonons have received further interest with the recent rise of nanomechanical resonators, widely used for sensing<sup>6</sup> or cavity optomechanics.<sup>7</sup> However, the measurement of these high-frequency phonons remains experimentally challenging. Indeed, with light scattering methods, a gap in the frequencies that can be investigated exists from a few tens of GHz with Brillouin light scattering to a few THz with x-ray scattering.<sup>8–10</sup> Picosecond ultrasonics,<sup>11</sup> a time domain approach to light scattering by phonons, has allowed bridging this gap.<sup>1–4</sup>

Picosecond ultrasonics is a technique based on ultrafast pump-probe spectroscopy to study the behavior of subterahertz to THz acoustic phonons in solid materials.<sup>8–10</sup> This technique is a powerful characterization tool used to investigate the numerous properties of

bulk and nanomaterials from elastic constants<sup>12,13</sup> to carrier diffusion.<sup>14</sup> The main detection mechanism in picosecond ultrasonics, the photoelastic mechanism, leads to the appearance of Brillouin oscillations, arising from the interference between optical pulses reflected by the sample interfaces and pulses scattered by acoustic phonons.<sup>1,15</sup> The study of Brillouin oscillation offers a wealth of information on the material properties. For example, the frequency is correlated with the refractive index and sound velocity.<sup>16</sup> Furthermore, the decay rate of the oscillations is indicative of the lifetime of acoustic phonons, which can allow the extraction of the attenuation factor.<sup>1,15</sup> However, in these characterizations, the effect of the probe pulse duration is seldom considered, despite its potential influence on signal loss. Indeed, the signal depends on the interference between the reflection of the probe pulses with different origins. Therefore, the temporal overlap of these reflections evolves in time and so does the amplitude of the signal. With the development of always shorter pulse, understanding the role played by the probe pulse duration is critical for the reliable extraction of material properties.

In this Letter, we investigate the effect of probe pulse duration on the lifetime of Brillouin oscillations in picosecond ultrasonics. We first

calculate how the probe pulse duration affects the decay of the signal. We highlight two regimes depending on the ratio of the probe pulse duration and material-related decay processes (phonon attenuation and probe absorption). For ultrashort pulses, the decay is dominated by the probe pulse duration, while for longer pulses, the signal loss is predominantly induced by material properties. We performed picosecond ultrasonics experiments on a GaAs substrate with a fixed pump pulse duration and a varying probe pulse duration and highlighted the existence of these regimes. We show that the extraction of reliable physical parameters, such as the penetration depth or phonon lifetime, is dependent on the knowledge of the probe pulse duration. Finally, we apply this principle to the investigation of the acoustic attenuation factor of  $\text{CH}_3\text{NH}_3\text{PbBr}_3$ , showcasing the strong anharmonicity of this material.

In picosecond ultrasonics, two femtosecond pulses generate and detect coherent acoustic phonons (CAPs). The absorption of the pump pulse leads to the generation of CAPs through various mechanisms<sup>9</sup> such as thermoelasticity or deformation potential. The propagation and dissipation of coherent acoustic phonons (CAPs) are detected through their interaction with the probe pulse.<sup>10</sup> When an incoming probe pulse interacts with the sample, it is partially reflected by the interfaces and the CAP wavepacket. These multiple reflections interfere and lead to the apparition of Brillouin oscillations in the transient reflectivity at the frequency  $f = \frac{2nv}{\lambda}$ , where  $n$  is the refractive index at the probe wavelength  $\lambda$  and  $v$  is the longitudinal sound velocity of the material.<sup>1,15</sup> Multiple effects are responsible for the decay of these oscillations, as depicted in Fig. 1.

For instance, phonon scattering, which leads to decoherence of the wavepacket, reduces the content of the acoustic pulse at the frequency of Brillouin oscillations and, consequently, the amount of reflected light by the CAPs [Fig. 1(a)]. The limited penetration depth of the probe pulse also leads to signal loss as the CAPs propagate within the sample. The small amount of probe light that reaches the CAPs that have propagated to the depth of the sample results in a decrease in the measured signal [Fig. 1(b)]. Finally, the mechanism of concern in this work is the diminishing overlap between the probe pulse reflected at the free surface and the one scattered by the CAPs. When the scattering of light by the phonons occurs far from the surface, the temporal overlap between the two reflected optical fields is reduced, and so is the signal [Fig. 1(c)]. The overlap is further reduced by the use of an ultrashort laser pulse.

To better quantify each effect, in the following, we derive the transient reflectivity, taking into account the probe pulse duration. For simplicity, we consider that the refractive index does not vary in the range of wavelengths contained in the probe pulse. We make this assumption to more clearly highlight the main mechanisms responsible for signal loss. However, in the simulations, we performed, and we took the dispersion of the refractive index into account. We also make the assumption that the acoustic strain can be assimilated as a Dirac delta function. We can justify this assumption by considering that the shortest probe pulse we use in this study has a duration of 23 fs, which corresponds to a spatial extent of  $6.9 \mu\text{m}$ , which is much larger than the CAPs' spatial extent dictated by the penetration depth of the pump pulse and that is on the order of 100 nm. The reflectivity induced by the scattering of the probe light at the pulsation  $\omega$  by the CAPs is, thus, given by<sup>10,17</sup>

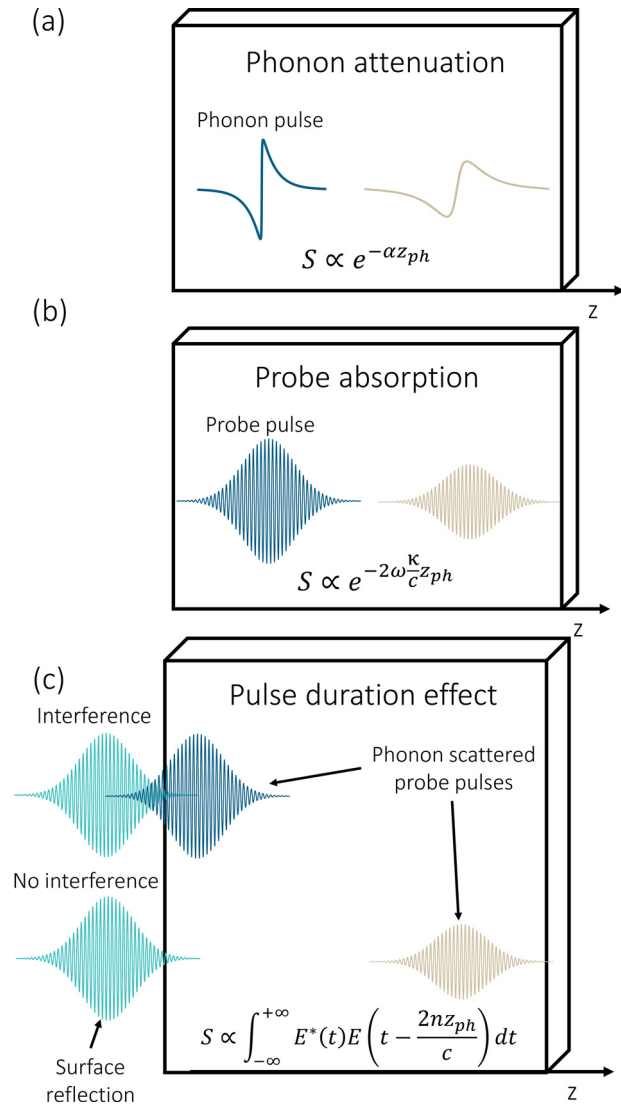


**FIG. 1.** Origin of signal decay in picosecond ultrasonics. (a) Decay of signal due to coherent phonon attenuation. As the coherent acoustic phonon wavepackets propagate through the material, they scatter, and their amplitudes are reduced, which leads to a decrease in the signal  $S$ . (b) Decay of signal due to the absorption of the probe pulse within the sample. As the coherent phonons propagate deeper into the sample, the probe light needs to travel a longer distance in the sample leading to a decrease in the signal. (c) Decay of the signal due to vanishing of the temporal overlap of the probe reflections. The signal is detected through the interference between the surface reflected probe pulse and the phonon scattered probe pulse. When the phonons propagate, the probe pulse needs to travel a longer distance, and the two reflections will not overlap temporally in the detector, which leads to a decrease in the signal.

$$\delta r = \frac{4ikn}{(1+n)^2} \frac{\partial \tilde{n}}{\partial \eta} e^{i\omega \frac{2nz_{ph}}{c}} e^{-\alpha z_{ph}} e^{-\frac{2\kappa z_{ph}}{c}}, \quad (1)$$

where  $k$  is the wavevector of light,  $c$  is the speed of light,  $\tilde{n} = n + i\kappa$  is the complex refractive index,  $\frac{\partial \tilde{n}}{\partial \eta}$  is the photoelastic coefficient,  $z_{ph}$  is the position of the CAPs, and  $\alpha$  is the acoustic attenuation factor.

We can divide this expression into various components that contribute differently to the evolution of the signal as the CAPs propagate. First, the term  $\frac{4ikn}{(1+n)^2} \frac{\partial n}{\partial \eta}$  is intrinsic to the photon-phonon interaction in the material and induces a constant change of phase and amplitude of the scattered probe light, regardless of the CAPs' position. In the following, we will write this term as  $\rho e^{j\theta}$ . The following term corresponds to a delay induced by the propagation of the probe pulse within the material before and after scattering with CAPs. It is this term that, when considering the limited probe pulse duration, participates to the signal loss, as depicted in Fig. 1(c). We then have a decaying exponential that is caused by the attenuation of the CAPs as they propagate within the medium. This mechanism is illustrated in Fig. 1(a). Finally, the last term corresponds to the absorption of the probe light within the material, shown in Fig. 1(b).

The electric field reflected by the sample is, thus, composed of two terms, the reflection at the free surface and the reflection by the CAPs. To obtain the reflected electric field in the time domain, we perform the inverse Fourier transform of the reflected monochromatic field [Eq. (1)], taking into account the spectral density of the pulse  $A(\omega)$ ,

$$rE(t) = \int_{-\infty}^{+\infty} d\omega A(\omega) \left( r_0 + \rho e^{j\theta} e^{-\alpha z_{ph}} e^{i\omega \frac{2(n+jk)z_{ph}}{c}} \right) e^{-j\omega t}. \quad (2)$$

This expression is the most general expression of the reflected electric field for a probe pulse of limited duration. Since we assumed the dispersion to be negligible for the wavelength range we consider here, we can rewrite this expression as

$$rE(t) = r_0 E_{pulse}(t) + \rho e^{j\theta} e^{-\alpha z_{ph}} e^{-i\omega \frac{2nz_{ph}}{c}} E_{pulse}\left(t - \frac{2nz_{ph}}{c}\right), \quad (3)$$

with

$$E_{pulse}(t) = \int_{-\infty}^{+\infty} d\omega A(\omega) e^{-j\omega t}. \quad (4)$$

In this expression, we notice that in the second term, the pulse has been shifted by  $\frac{2nz_{ph}}{c}$ , which corresponds to the additional propagation in the sample before and after scattering with the CAPs.

Finally, in the case of monochromatic plane waves, the transient reflectivity is given by  $2Re\delta r/r_0$ .<sup>10</sup> To take into account the pulse nature of the probe, we need to integrate this quantity over time, which naturally occurs in the photodetector

$$\Delta R(z_{ph}) \propto e^{-\alpha z_{ph}} e^{-i\omega \frac{2nz_{ph}}{c}} Re \left( \int_{-\infty}^{\infty} dt E_{pulse}^*(t) E_{pulse}\left(t - \frac{2nz_{ph}}{c}\right) e^{j\theta} \right). \quad (5)$$

In this expression, we have only kept the terms corresponding to the loss of the signal. The first two exponential terms have been explained previously and correspond to acoustic attenuation and optical absorption, respectively. The last term is usually not appearing in picosecond ultrasonic treatment, because relatively long optical pulses (on the order of a few hundred femtoseconds) are considered. This term is the field autocorrelation, and it induces another decay component to the signal. Indeed, as the CAPs propagate deeper into the sample, the probe pulse reflected by the CAPs is getting increasingly delayed with respect to the reflection at the free surface. As the delay

becomes longer than the probe pulse duration, the two reflections do not overlap temporally in the detector, which leads to a null field autocorrelation. For extremely short pulses, this decay mechanism becomes the predominant one. It is also interesting to note that for decay due to material properties, namely, phonon attenuation and optical absorption, we have an exponential decay, while for the signal loss due to the limited probe pulse duration, the decay follows the shape of the autocorrelation. In our case, we consider a Gaussian pulse, and the decay due to the probe duration follows a Gaussian shape.

To investigate experimentally the effect of probe pulse duration, picosecond ultrasonics experiments were performed in a reflection scheme as depicted in Fig. 2(a). A regeneratively amplified, mode-locked Yb:KGW (potassium gadolinium tungstate) laser system was used to pump two non-collinear optical parametric amplifiers (NOPAs). One of the NOPAs generated the pump pulses and the other one generated the probe pulses at variable wavelengths. The probe pulse duration was varied from 20 to 90 fs using a prism compressor at the output of the NOPA. The probe pulse duration was extracted by performing the autocorrelation of the pulses. After the compressor, the probe pulse goes through a mechanical delay line and

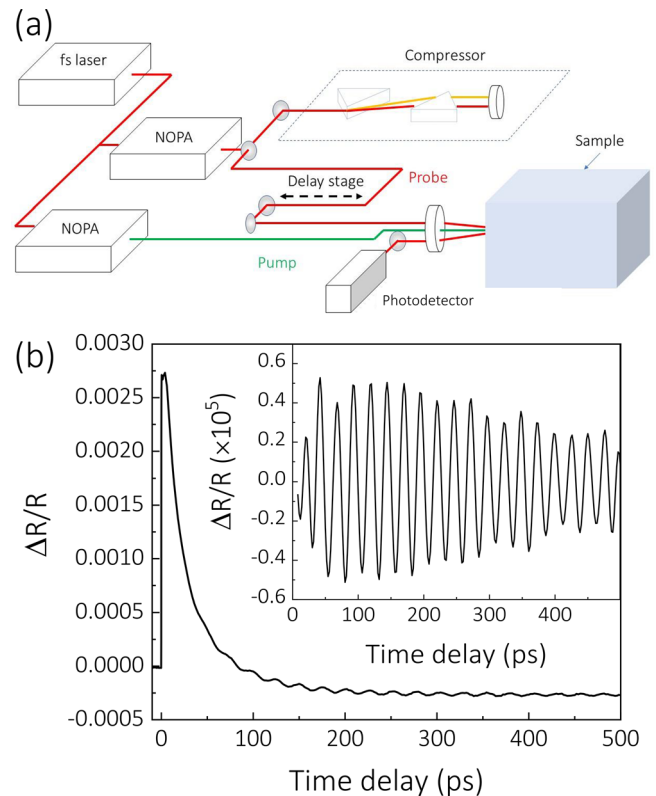


**FIG. 2.** Picosecond ultrasonics. (a) Schematic representation of a picosecond ultrasonic experiment. A femtosecond laser is sent into two NOPAs to generate the pump and probe pulse. Using a prism compressor, we can control the duration of the probe pulse. In this setup, the pump beam is absorbed by the sample and generates coherent acoustic phonons, and the probe is time delayed and monitors the evolution of the strain wave. (b) Transient reflectivity measurement obtained on the GaAs substrate for a pump beam of duration 22 fs and wavelength centered at 550 nm and a probe beam of duration 90 fs and a wavelength centered at 880 nm.

reaches the sample at normal incidence. The reflection is collected in a photodetector, and its temporal evolution is monitored.

Figure 2(b) shows a signal measured on a GaAs substrate for a pump wavelength of 550 nm and duration 22 fs and a probe pulse of 90 fs duration at a wavelength of 880 nm. On this signal, we first observe a sharp increase in the reflectivity induced by photoexcitation of electrons. The signal then decays toward its equilibrium value through various relaxation processes. Superimposed on this trace are Brillouin oscillations. The inset of Fig. 2 shows these oscillations after removing the electronic and thermal (incoherent phonons) components. This procedure may lead to an artifact in the oscillations at early timescales; thus, we should only consider the decay after the signal reached its maximum value. We measure a frequency of 38.5 GHz in good agreement with the calculated value of 38.4 GHz using a sound velocity of  $4730 \text{ m s}^{-1}$  and a refractive index of 3.57.<sup>18</sup>

In Fig. 3, we show how the Brillouin oscillations are affected by the probe pulse duration. We show the oscillatory components of the transient reflectivity for three different probe pulse durations of 27, 52, and 90 fs and a fixed pump duration of 22 fs.

We observe that as the probe duration of the pulse increases, so does the lifetime of Brillouin oscillations. In other words, the pulse autocorrelation decays faster than the signal losses due to material properties, and we are in the regime where the lifetime is at least partly determined by the probe pulse duration. We modeled the Brillouin oscillations signal using Eq. (5), but taking into consideration the dispersion of optical properties in the wavelength range of the probe. The fitting parameters are the phase  $\theta$  and the acoustic attenuation factor  $\alpha$ , which are uniquely determined for all experiments. For each probe pulse duration, we obtain excellent agreement, which highlights the fact that for ultrashort pulses, the signal decay is dictated by the pulse autocorrelation function. For the shortest pulse, the frequency content of the pulse becomes richer, and the increased absorption of wavelengths close to the bandgap of GaAs could induce a decay of the signal. We performed additional simulations for this probe pulse duration, where we neglected optical absorption and did not observe any noticeable difference, which confirm the major role played by the pulse autocorrelation function.

The fact that the probe pulse duration is the main mechanism for signal loss indicates that the measurement of phonon lifetime using the decay of the Brillouin oscillations is not reliable, and we can only obtain an upper bound of the acoustic attenuation factor. Using longer probe pulses, we can refine the value of this upper bound, and for the probe pulse duration of 90 fs, we obtain  $0.05 \mu\text{m}^{-1}$ . This value is larger than the reported value of  $0.04 \mu\text{m}^{-1}$  for 56 GHz phonons at room temperature measured by observing the decay of successive echoes.<sup>2</sup> These two attenuation factors correspond to different phonon frequencies; but, considering that in GaAs, attenuation follows a  $\omega^2$  law,<sup>4</sup> we would expect the attenuation factor at 38.5 GHz to be smaller than at 56 GHz, which indicates that the attenuation is overestimated and that measuring the attenuation of hypersonic waves through the lifetime of Brillouin oscillations is not a reliable approach for sub-100 fs pulses.

To show the generality of these findings, we performed similar experiments on  $\text{CH}_3\text{NH}_3\text{PbBr}_3$  with a pump wavelength of 400 nm and a duration of 32 fs, and a probe wavelength of 600 nm and a duration of either 23 or 80 fs, as shown in Fig. 3(b). We observe oscillations at a frequency of 21.6 GHz. Assuming a refractive index value of 2.1,<sup>19</sup> we obtain a sound velocity of  $3085 \text{ m s}^{-1}$ , in good agreement with the

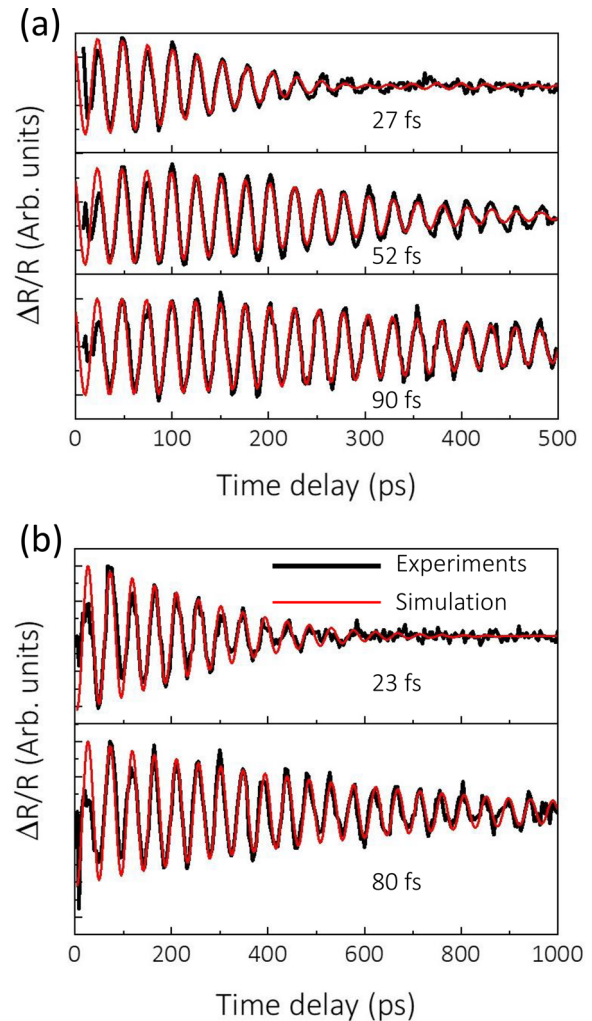


**FIG. 3.** Probe pulse duration dependent lifetime. (a) Brillouin oscillations measured in GaAs for a probe wavelength of 880 nm and a varying pulse duration of either 27, 52, or 90 fs, and simulation of these data using Eq. (5). (b) Brillouin oscillations measured in  $\text{CH}_3\text{NH}_3\text{PbBr}_3$  for a probe wavelength of 600 nm and a varying pulse duration of either 23 or 80 fs, and simulation of these data using Eq. (5).

literature.<sup>20</sup> As in the case of GaAs, the observed lifetime depends on the probe pulse duration. We can deduce that the upper bound of the attenuation factor of  $\text{CH}_3\text{NH}_3\text{PbBr}_3$  at 21.6 GHz is  $0.5 \mu\text{m}^{-1}$ , which is an order of magnitude higher than for GaAs. The attenuation factor represents how strongly phonons at 21.6 GHz scatter with other phonons, electrons, interfaces, and defects and, therefore, lose their energy. The interaction of the 21.6 GHz phonons with other phonons is responsible for the anharmonicity of the crystal. As our  $\text{CH}_3\text{NH}_3\text{PbBr}_3$  sample is a single crystal, the role played by interfaces and grain boundaries is limited; thus, we consider that the attenuation factor is representative of the scattering with other phonons and defects inside the materials.

In the recent decades, halide perovskites have been intensively studied for their exceptional photovoltaic performance. A wide range



of mechanisms explaining this performance are related to the anharmonicity of these materials such as carrier mobility<sup>23</sup> and polaron formation.<sup>24</sup> Assuming that the attenuation factor measured in  $\text{CH}_3\text{NH}_3\text{PbBr}_3$  directly reflects the anharmonicity of this material,<sup>21,22</sup> we find that the attenuation factor is at least an order of magnitude larger than GaAs. Our study shows that transport properties in  $\text{CH}_3\text{NH}_3\text{PbBr}_3$  and halide perovskites, in general, need to account for the soft nature of these materials.

In conclusion, we have investigated the role played by the probe pulse duration in the decay of Brillouin oscillations in picosecond ultrasonics. We first derive a model to calculate the transient reflectivity induced by propagating coherent acoustic phonons in the case of ultrashort probe pulses. We show that for short pulse duration, Brillouin oscillations decay as the autocorrelation of the probe pulse and the signal disappears because of the vanishing temporal overlap of the probe pulse reflected at the free surface and the one reflected by the phonons. We then verified experimentally this model for a GaAs substrate and were able to extract an upper limit of acoustic attenuation for 38.5 GHz at  $0.05\ \mu\text{m}^{-1}$  and apply similar concepts to  $\text{CH}_3\text{NH}_3\text{PbBr}_3$  to obtain an acoustic attenuation of  $0.5\ \mu\text{m}^{-1}$  at 21.6 GHz. Our result shows that for a reliable extraction of the lifetime of phonons using Brillouin oscillations, it is crucial to take into account the effect of the probe pulse duration.

This work was supported by NanoLund, Lunds Universitet, Lund Laser Centre, Crafoordska Stiftelsen, Grant No. 20200630, Vetenskapsrådet, Grant No. 2017-05150, and China Sponsorship Council, Grant No. 201506360083.

## AUTHOR DECLARATIONS

### Conflict of Interest

The authors have no conflicts to disclose.

### DATA AVAILABILITY

The data that support the findings of this study are available from the corresponding authors upon reasonable request.

## REFERENCES

- P. Emery and A. Devos, "Acoustic attenuation measurements in transparent materials in the hypersonic range by picosecond ultrasonics," *Appl. Phys. Lett.* **89**, 191904 (2006).
- W. Chen, H. J. Maris, Z. R. Wasilewski, and S.-I. Tamura, "Attenuation and velocity of 56 GHz longitudinal phonons in gallium arsenide from 50 to 300 K," *Philos. Mag. B* **70**, 687–698 (1994).
- P.-A. Mante, C.-C. Chen, Y.-C. Wen, J.-K. Sheu, and C.-K. Sun, "Thermal boundary resistance between GaN and cubic ice and THz acoustic attenuation spectrum of cubic ice from complex acoustic impedance measurements," *Phys. Rev. Lett.* **111**, 225901 (2013).
- R. Legrand, A. Huynh, B. Jusserand, B. Perrin, and A. Lemaître, "Direct measurement of coherent subterahertz acoustic phonons mean free path in GaAs," *Phys. Rev. B* **93**, 184304 (2016).
- B. Rufflé, D. A. Parshin, E. Courtens, and R. Vacher, "Boson peak and its relation to acoustic attenuation in glasses," *Phys. Rev. Lett.* **100**, 015501 (2008).
- J. Chaste, A. Eichler, J. Moser, G. Ceballos, R. Rurali, and A. Bachtold, "A nanomechanical mass sensor with yoctogram resolution," *Nat. Nanotechnol.* **7**, 301–304 (2012).
- M. Aspelmeyer, T. J. Kippenberg, and F. Marquardt, "Cavity optomechanics," *Rev. Mod. Phys.* **86**, 1391–1452 (2014).
- A. Devos, M. Foret, S. Ayrinhac, P. Emery, and B. Rufflé, "Hypersound damping in vitreous silica measured by picosecond acoustics," *Phys. Rev. B* **77**, 100201 (2008).
- P. Ruello and V. E. Gusev, "Physical mechanisms of coherent acoustic phonons generation by ultrafast laser action," *Ultrasonics* **56**, 21–35 (2015).
- O. Matsuda, M. C. Larciprete, R. L. Voti, and O. B. Wright, "Fundamentals of picosecond laser ultrasonics," *Ultrasonics* **56**, 3–20 (2015).
- C. Thomsen, H. T. Grahn, H. J. Maris, and J. Tauc, "Surface generation and detection of phonons by picosecond light pulses," *Phys. Rev. B* **34**, 4129–4138 (1986).
- P.-A. Mante, S. Lehmann, N. Anttu, K. A. Dick, and A. Yartsev, "Nondestructive complete mechanical characterization of zinc blende and wurtzite GaAs nanowires using time-resolved pump-probe spectroscopy," *Nano Lett.* **16**, 4792–4798 (2016).
- P. A. Mante, J. F. Robillard, and A. Devos, "Complete thin film mechanical characterization using picosecond ultrasonics and nanostructured transducers: Experimental demonstration on  $\text{SiO}_2$ ," *Appl. Phys. Lett.* **93**, 071909 (2008).
- O. B. Wright, B. Perrin, O. Matsuda, and V. E. Gusev, "Ultrafast carrier diffusion in gallium arsenide probed with picosecond acoustic pulses," *Phys. Rev. B* **64**, 081202 (2001).
- H. Ogi, T. Shagawa, N. Nakamura, M. Hirao, H. Odaka, and N. Kihara, "Elastic constant and Brillouin oscillations in sputtered vitreous  $\text{SiO}_2$  thin films," *Phys. Rev. B* **78**, 134204 (2008).
- R. Côté and A. Devos, "Refractive index, sound velocity and thickness of thin transparent films from multiple angles picosecond ultrasonics," *Rev. Sci. Instrum.* **76**, 053906 (2005).
- K. Lai, D. Finkelstein-Shapiro, S. Lehmann, A. Devos, and P.-A. Mante, "Fano resonance between Stokes and anti-Stokes Brillouin scattering," *Phys. Rev. Res.* **3**, L032010 (2021).
- S. Adachi, "Optical dispersion relations for GaP, GaAs, GaSb, InP, InAs, InSb,  $\text{Al}_x\text{Ga}_{1-x}\text{As}$ , and  $\text{In}_{1-x}\text{Ga}_x\text{As}_y\text{P}_{1-y}$ ," *J. Appl. Phys.* **66**, 6030–6040 (1989).
- S. Brittman and E. C. Garnett, "Measuring  $n$  and  $k$  at the microscale in single crystals of  $\text{CH}_3\text{NH}_3\text{PbBr}_3$  perovskite," *J. Phys. Chem. C* **120**, 616–620 (2016).
- J. Feng, "Mechanical properties of hybrid organic-inorganic  $\text{CH}_3\text{NH}_3\text{BX}_3$  ( $\text{B} = \text{Sn}$ ,  $\text{Pb}$ ;  $\text{X} = \text{Br}$ ,  $\text{I}$ ) perovskites for solar cell absorbers," *APL Mater.* **2**, 081801 (2014).
- T. Debnath, D. Sarker, H. Huang, Z.-K. Han, A. Dey, L. Polavarapu, S. V. Levchenko, and J. Feldmann, "Coherent vibrational dynamics reveals lattice anharmonicity in organic-inorganic halide perovskite nanocrystals," *Nat. Commun.* **12**, 2629 (2021).
- K. Ishioka, T. Tadano, M. Yanagida, Y. Shirai, and K. Miyano, "Anharmonic organic cation vibrations in the hybrid lead halide perovskite  $\text{CH}_3\text{NH}_3\text{PbI}_3$ ," *Phys. Rev. Mater.* **5**, 105402 (2021).
- A. D. Wright, C. Verdi, R. L. Milot, G. E. Eperon, M. A. Pérez-Osorio, H. J. Snaith, F. Giustino, M. B. Johnston, and L. M. Herz, "Electron-phonon coupling in hybrid lead halide perovskites," *Nat. Commun.* **7**, 11755 (2016).
- J. M. Frost, L. D. Whalley, and A. Walsh, "Slow cooling of hot polarons in halide perovskite solar cells," *ACS Energy Lett.* **2**, 2647–2652 (2017).